RPA: Tool for Rocket Propulsion Analysis

Thermal Analysis of Thrust Chambers

Alexander Ponomarenko

contact@propulsion-analysis.com

http://www.propulsion-analysis.com

June 2012

Abstract

RPA (Rocket Propulsion Analysis) is a multi-platform analysis tool intended for use in conceptual and preliminary design of rocket engines.

This article describes a numerical model of thermal analysis of cooled combustion chambers and nozzles, implemented as a Thermal Analysis Module for RPA.

Contents

Nomenclature

τ	viscosity stress
q	heat flux
α_T	heat transfer coefficient
Re	Reynolds number
Pr	Prandtl number
μ , μ_t	laminar and turbulent coefficient of viscosity
A	area, m^2
p	pressure, Pa
T	temperature, K
w	velocity, m/s
ρ	density, kg/m^3
V	volume, m^3
$\dot{m}$	mass flow rate
λ_w	thermal conductivity
I_s	specific impulse, m/s
$c*$	characteristic exhaust velocity, m/s
C_F	thrust coefficient
ξ_f	friction loss coefficient
φ_f	performance correction factor for the friction loss

Further symbols will be introduced and explained in the text.

Introduction

Thermal analysis is an essential part in the design of rocket engines. The rapid and accurate estimation of cooling effectiveness is required if new vehicle propulsion concepts are to be evaluated in a timely and cost effective manner. The used tools should allow the analysis of different types of cooling methods, including radiation, convective and film cooling.

Numerical model described in this article and implemented in RPA enables the thermal analysis of rocket engine thrust chambers with accuracy sufficient for conceptual and preliminary design studies, as well as for rapid evaluation of different variants of cooled thrust chambers and its verification in detailed design phase.

Numerical Model

Gas-Side Heat Transfer

The thermodynamic and transport properties of the combustion gases are evaluated using the chemical equilibrium composition module of the RPA [9].

Ievlev's Method

Ievlev obtained the gas-side heat flux calculation method from integral boundary layer equations and semi-empirical heat transfer relations. The detailed description of the method as well as derivation of relations can be found in [1].

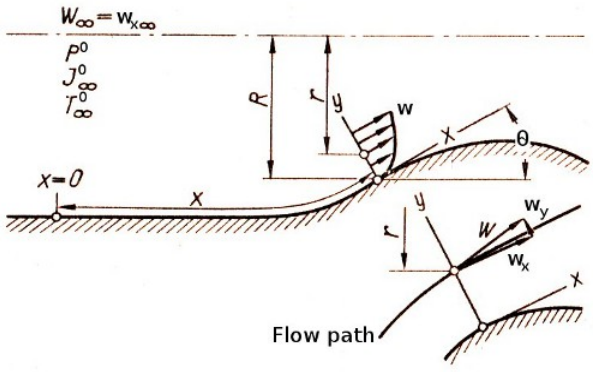

Figure 1: Definition sketch for flow in boundary layer

Assuming that there is no chemical reaction in the boundary layer, the governing equations for boundary layer in axisymmetric channel (see figure 1) are given as follows:

the continuity equation:

$$\frac{\partial}{\partial x}(r\rho w_x) + \frac{\partial}{\partial x}(r\rho w_y) = 0$$

the momentum equation:

$$\rho w_x \frac{\partial w_x}{\partial x} + \rho w_y \frac{\partial w_y}{\partial y} = -\frac{dp}{dx} + \frac{1}{r}\frac{\partial}{\partial y}(r\tau)$$

the energy equation:

$$\rho w_x \frac{\partial I^0}{\partial x} + \rho w_y \frac{\partial I^0}{\partial y} = -\frac{1}{r}\frac{\partial}{\partial y}(r q)$$

where

$$\tau = (\mu + \mu_t)\frac{\partial w_x}{\partial y} \quad \text{and} \quad q = \frac{\lambda + \lambda_t}{c_p}\frac{\partial I^0}{\partial y} \quad .$$

Integrating these equations yield:

$$\frac{d}{dx}(\rho_x w_\infty^2 \delta^{**} R) + \frac{dw_\infty}{dx}(\rho_\infty w_\infty \delta^* R) = \tau_w R$$

$$\frac{d}{dx}[\rho_x w_\infty (I_\infty^0 - I_w)\delta_T^{**} R] = q_w R$$

where

$$\delta^* = \int_0^\infty \frac{r}{R}\left(1 - \frac{\rho w_x}{\rho_\infty w_\infty}\right) dy$$

$$\delta^{**} = \int_0^\infty \frac{\rho w_x r}{\rho_\infty w_\infty R}\left(1 - \frac{w_x}{w_\infty}\right) dy$$

$$\delta_T^{**} = \int_0^\infty \frac{\rho w_x r}{\rho_\infty w_\infty R}\frac{I_\infty^0 - I^0}{I_\infty^0 - I_w} dy$$

Introducing new variables:

$$\mathrm{Re}^{**} = \frac{\rho_x w_\infty \delta^{**}}{\mu_x} \quad ; \quad \mathrm{Re}_T^{**} = \frac{\rho_x w_\infty \delta_T^{**}}{\mu_x} \quad ; \quad \mathrm{Re}^0 = \frac{\rho_\infty^0 w_{max} D_t}{\mu_\infty^0}$$

and

$$\alpha = \frac{\tau_w}{\rho_x w_\infty^2} \quad ; \quad \alpha_T = \frac{q_w}{\rho_x w_\infty (I_\infty^0 - I_\infty)}$$

as well as

$$z = \frac{\mathrm{Re}^{**}}{\alpha} \qquad z_T = \frac{\mathrm{Re}_T^{**}}{\alpha_T}$$

and making some generalizations from empirical data, Ievlev obtained the following

correlations:

$$\frac{z_T}{z}=\left(1.769\,\frac{1-\beta^2+\beta^2\left(1-0.08696\,\dfrac{1-\beta^2}{1-\bar{T}_w+0.1\beta^2}\right)}{1-\bar{T}_w+0.1\beta^2}\right)^{0.54} \qquad 1.1$$

$$z_T=\frac{\mathrm{Re}_0}{(1-\gamma)\bar{D}^{\frac{1}{1-\gamma}}(I^0_\infty-I_w)^{\frac{1}{1-\gamma}}}\int_{l_0}^{\bar{l}}\frac{\rho_x}{\rho^0_\infty}\frac{\mu^0_\infty}{\mu_x}\bar{D}^{\frac{1}{1-\gamma}}(I^0_\infty-I_w)^{\frac{1}{1-\gamma}}\beta\frac{d\,\bar{l}}{\cos\theta}\ +\ const \qquad 1.2$$

$$\alpha_T=\frac{\left(\dfrac{z}{z_T}\right)^{0.089\,Pr^{-0.56}}\left(1-0.21\,\dfrac{1-Pr}{Pr^{4/3}}\,\dfrac{\beta^2}{1-\bar{T}_w}\right)^{0.9225}}{\left(307.8+54.8\log^2\left(\dfrac{Pr}{19.5}\right)\right)Pr^{0.45}\,z^{0.08}-650} \qquad 1.3$$

$$\alpha=0.03327\mathrm{z}^{-0.224}+3.966\cdot10^{-4} \qquad 1.4$$

$$q_w\ =\ \alpha_T\rho_x w_\infty(I^0_\infty-I_w) \qquad 1.5$$

$$\tau_w\ =\ \alpha\rho_x w^2_\infty \qquad 1.6$$

where

$\beta=w/w_{max}$, $w_{max}=\sqrt{2\gamma(RT)^0_\infty/\gamma-1}$

$\bar{T}_w=T_w/T_e$, $T_e=R\,T^0_\infty/R_{1500}$, R_{1500} - gas constant of reaction products at $T=1500\,K$

$\bar{D}=D/D_t=2\mathrm{R}/D_t$, $l=l/D_t$

$$\frac{\rho_x}{\rho^0_\infty}=\frac{p}{p^0_c}\left(\frac{1+\bar{T}_w}{2}-\frac{\beta^2}{4}\right)^{-0.823}\left(\frac{3+\bar{T}_w}{4}-\frac{9\beta^2}{16}\right)^{-0.177}$$

$$\frac{\mu^0_\infty}{\mu_x}\approx\left(\frac{1+\bar{T}_w}{2}-\frac{\beta^2}{4}\right)^{-0.7}$$

Using these relations, the heat flux is calculated as follows:

1. Subdivide the thrust chamber into several stations (see figure 2).
2. Assign the wall temperature to each station (when calculation chamber cooling, use the results from the previous iteration).
3. Using chemical equilibrium composition module of the RPA [9], calculate the hot gas properties at each station.
4. Using relations 1.1 and 1.2, calculate values of z and z_T at each station.

5. From equation 1.3, calculate the heat transfer coefficient α_T .
6. From equation 1.5, calculate the heat flux q .
7. Calculate the viscosity stress τ , using equations 1.4 and 1.6.

The following approach is used to calculate the value of $I_\infty^0 - I_w$ (as described in [2]):

$T_\infty^0 > 1500\,K$ and $T_w < 1500\,K$:

- I_∞^0 is calculated as a stagnation enthalpy in combustion chamber
- I_w is calculated as enthalpy of reaction products at the temperature T_w , but with composition that corresponds to the temperature 1500 K.

$T_\infty^0 > 1500\,K$ and $T_w > 1500\,K$:

- I_∞^0 is calculated as a stagnation enthalpy in combustion chamber
- I_w is calculated as enthalpy of reaction products at the temperature T_w , but with composition that corresponds to the temperature 1500 K.

Bartz Method

The basic correlation for gas-side heat transfer is given by

$$q_w = \alpha_T (T_e - T_w)$$

where

$$T_e = T_c^0 \left[\frac{1 + Pr^{0.33} \left(\frac{\gamma - 1}{2} \right) M^2}{1 + \left(\frac{\gamma - 1}{2} \right) M^2} \right]$$

For the heat transfer coefficient, the following correlation is used [3]:

$$\alpha_T = \left[\frac{0.026}{D_t^{0.2}} \frac{(\mu_\infty^0)^{0.2} c_{p\infty}^{\,0}}{(Pr_\infty^0)^{0.6}} \left(\frac{p_c^0}{c^*} \right)^{0.8} \left(\frac{D_t}{R} \right)^{0.1} \right] \left(\frac{A_t}{A} \right)^{0.9} \sigma$$

The correction factor σ can be calculated as follows:

$$\sigma = \left[\frac{1}{2} \frac{T_w}{T_c^0} \left(1 + \frac{\gamma - 1}{2} M^2 \right) + \frac{1}{2} \right]^{-0.68} \left[1 + \frac{\gamma - 1}{2} M^2 \right]^{-0.12}$$

Boundary Layer Cooling

The analysis method for estimation of boundary layer cooling effectiveness is developed under the following assumptions:

- the large-scale distribution of mixture composition and the gas properties in the shear flow are conserved along the nozzle;
- the convective heat flux to the wall is completely defined by the heat transfer between the wall and the layer next to the wall
- the layer next to the wall is transparent for the radiation heat transfer

To calculate the convective heat flux from the cooler surface layer, the Ievlev's correlation for similar conditions is used:

$$\frac{q^{(1)}}{q^{(2)}} = \frac{S^{(1)}}{S^{(2)}}$$

where

$$S = \frac{(I_{\infty}^{0} - I_{w}) T_{e}^{0.425} \mu_{1000}^{0.15}}{R_{1500}^{0.425} (T_{e} + T_{w})^{0.595} (3T_{e} + T_{w})^{0.15}}$$

Using these correlation, the heat flux is calculated as follows:

1. Calculate the heat flux $q^{(1)}$ to the wall from the core flow (that is, without taking into account the presence of the cooler surface layer)
2. Calculate the value $S^{(1)}$ for the gas in the flow core
3. For the known mixture composition within the surface layer, calculate the parameters of the gas in this layer, using the chemical equilibrium composition module of the RPA [9]
4. Calculate the value $S^{(2)}$ for the gas in the surface layer
5. Calculate the corrected heat flux as $q^{(2)} = q^{(1)} \frac{S^{(2)}}{S^{(1)}}$

Film Cooling

Gaseous Film

After injecting into the thrust chamber, the gaseous coolant is mixing with existing surface layer and producing the layer with new mixture composition.

Correlations for the turbulent mixing are developed from [1] and given by

$$(r_i)_s = k_{ss}(r_i)_s^0 + k_{sf}(r_i)_f^0 \quad (i=0...NS)$$

$$(r_i)_f = k_{fs}(r_i)_s^0 + k_{ff}(r_i)_f^0 \quad (i=0...NS)$$

$$k_{ss}=\frac{\bar{m}_s^0}{\bar{m}_s}\left(1-\frac{\xi}{2}\right) \quad , \quad k_{sf}=\frac{\bar{m}_f^0}{\bar{m}_s}\frac{\xi}{2}$$

$$k_{ff}=\frac{\bar{m}_f^0}{\bar{m}_f}\left(1-\frac{\xi}{2}\right) \quad , \quad k_{fs}=\frac{\bar{m}_s^0}{\bar{m}_f}\frac{\xi}{2}$$

$$\bar{m}_s=\bar{m}_s^0\left(1-\frac{\xi}{2}\right)+\bar{m}_f^0\frac{\xi}{2}$$

$$\bar{m}_f=\bar{m}_s^0\frac{\xi}{2}+\bar{m}_f^0\left(1-\frac{\xi}{2}\right)$$

$$\xi=1-e^{-M\bar{x}^2}$$

$$M=K_t\frac{\bar{m}_s}{\bar{m}_f}$$

$$\bar{x}^2=x/H_s$$

where

superscript “0” denotes the initial parameters of the surface layer and the film at the location of injection

subscripts “s” and “f” denote the parameters of the surface layer and the film correspondingly

NS – total number of species in the surface layer and the film (the initial composition of the coolant may differ from the initial composition of the surface layer)

r_i – mass ratio of the species i in the mixture

$\bar{m}_{s,f}=\frac{\dot{m}_{s,f}}{\dot{m}}$ – relative mass flow rate

$\dot{m}_f$ – mass flow rate of the coolant in the film

$\dot{m}_s$ – mass flow rate of the gas in the surface layer

$\dot{m}$ – total mass flow rate in the chamber

x – distance from the location of the film injection

H_s – thickness of the surface layer

$K_t = (0.05 \ldots 0.20) \cdot 10^{-2}$ – coefficient that reflects the intensity of the turbulent mixing

The mixture composition of the surface layer after mixing with gaseous film is determined via a space-marching technique starting from the location of coolant injection ($\xi = 0$) to the location where the coolant is completely mixed with the surface layer ($\xi = 1$).

The estimation of the cooling effectiveness at each station can be performed using Ievlev's correlation for similar conditions, as described in the previous section.

Liquid Film

When injected into the thrust chamber, the liquid coolant transformation goes through 3 phases:

- ***Heating***

  Assuming that the thin liquid coolant film is transparent for the radiation heat transfer, the only component of the total heat flux reaching the wall is the radiation heat flux, whereas the convective component heats the liquid coolant. The convective heat transfer from the liquid coolant to the wall may be neglected.

  The heating equation is given by

$$d T_f = \frac{2 \pi R \, q_w^{T_f}}{\eta \dot{m}_f \bar{c}_f} dx$$

  where

  $d T_f$ – increase in temperature of the coolant

  η – coefficient that reflects the stability of the liquid film and depends on Reynolds number calculated from the parameters of the liquid film (see figure 2)

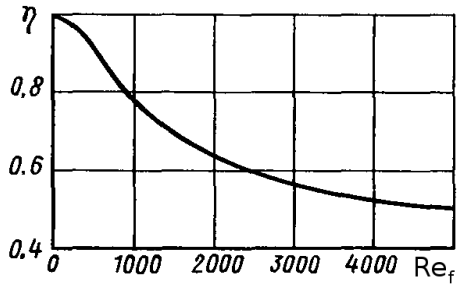

Figure 2: Film stability coefficient [1]

  $\mathrm{Re}_f = \frac{\dot{m}_f}{2 \pi R \mu_f}$ – Reynolds number calculated from the parameters of the liquid film

  $q_w^{T_f}$ – convective heat flux to the liquid coolant film at the coolant temperature T_f

  $\dot{m}_f$ – mass flow rate of the coolant in the film

  μ_f – viscosity of the coolant

  $\bar{c}_f$ – average specific heat of the coolant

  R , dx – size parameters of the chamber (see figure 1)

The heating of the film coolant is determined via a space-marching technique starting from the location of coolant injection to the location where the coolant is heated up to the temperature of vaporization or decomposition.

– ***Vaporization***

After heating up to vaporization/decomposition temperature, the part or all liquid in the film is vaporized. Similar to the heating, the convective heat transfer from the liquid coolant to the wall may be neglected.

The vaporization rate of the coolant is given by equation

$$d\dot{m}_f = \frac{2\pi R q_w^{T_{vap}}}{Q_{vap}} dx$$

where

$d\dot{m}_f$ – rate of the coolant vaporization/decomposition

$\dot{m}_f$ – mass flow rate of the coolant in the film

$q_w^{T_{vap}}$ – convective heat flux to the liquid coolant film at the coolant vaporization temperature T_{vap}

R , dx – size parameters of the chamber (see figure 1)

Q_{vap} – coolant heat of vaporization or decomposition

The vaporization or decomposition of the film coolant is determined via a space-marching technique starting from the location where the coolant reaches the temperature of vaporization or decomposition, to the location where the whole coolant is completely vaporized or decomposed.

– ***Mixing with surface layer***

The gaseous products of vaporization/decomposition are mixing with existing surface layer, producing the layer with new mixture composition. The mixing itself and the estimation of the boundary layer cooling effectiveness can be performed as described in two previous sections.

Radiation Heat Transfer

For given hot gas temperature T_∞ and wall temperature T_w , the basic correlation for the radiation heat transfer (under some assumptions mentioned in [1]) is given by

$$q_r = \varepsilon_e \sigma \left(\varepsilon_r^{T_\infty} T_\infty^4 - \varepsilon_g^{T_w} T_w^4 \right)$$

where

$\sigma = 5.670373 \times 10^{-8}$ $W/(m^2 K^4)$ – Stefan–Boltzmann constant;

$\varepsilon_e = \varepsilon_w / [1 - (1 - \varepsilon_w)(1 - \varepsilon_r^{T_w})]$ – effective emissivity coefficient of the wall;

ε_w – emissivity coefficient of the wall material (see Table 1 for typical values of some materials);

$\varepsilon_r^{T_\infty}$ – emissivity coefficient of the reaction products at temperature T_∞

$\varepsilon_r^{T_w}$ – emissivity coefficient of the reaction products at temperature T_w

Emissivity coefficients of reaction products at specific temperature T can be estimated as follows [2]:

$$\varepsilon_r^T = \sum_j \sum_i \beta_j [1 - \exp(-\langle K_{i,j} \rangle p_j L)] \frac{R^0_{\Delta\omega\, i,j}}{\sigma T^4}$$

where

j – molecule, *i* – radiation strip (see the table 2)

$$\langle K \rangle = \frac{\alpha_{3000}}{\Delta\omega} \frac{3000}{T}$$

$$R^0_{\Delta\omega} = \int_{\omega_1}^{\omega_2} \frac{3.742(\omega/1000)^3 \cdot 10^{-3}}{\exp(1.44\omega/T) - 1} d\omega$$

$\delta = 1$: $\omega_1 = \omega_0 - \Delta\omega/2$; $\omega_2 = \omega_0 + \Delta\omega/2$

$\delta = 0$: $\omega_1 = \omega_0 - (\Delta\omega - \Delta\omega_s)$; $\omega_2 = \omega_0 + \Delta\omega_s$

$\Delta\omega = \Delta\omega_s(1 - \delta) + a(1 + \delta)(T/1000)^{0.5}$

$\beta_{H2O} = 1.09$, $\beta_{j!=H2O} = 1.00$

$L = 0.9 \frac{4V}{F}$, where V and F – the volume and surface area of combustion chamber.

Table 1. Emissivity coefficients of some materials [4]

Material	Surface temperature Tw, K	Emissivity coefficient
Aluminum, oxidized	450 – 850	0.11 – 0.19
Copper alloy (bronze), polished	320	0.1
Copper alloy (bronze), rough	320 – 420	0.55
Copper alloy (brass), oxidized	450 – 850	0.61 – 0.59

Copper, oxidized	450 – 850	0.57 – 0.87
Nickel, oxidized	450 – 850	0.37 – 0.48
Niobium	450 – 650 1250 – 1850	0.17 0.20
Stainless steel	750	0.35
Steel, oxidized	450 – 850	0.8
Steel, heavily oxidized	750	0.98
Chrom-Nickel alloy	400 – 1300	0.64 – 0.76

Table 2. Data for calculation of emissivity coefficients of reaction products [2]

Parameter	$H_2O(1)$	$H_2O(2)$	$H_2O(3)$	$H_2O(4)$	$H_2O(5)$	$OH(1)$	$OH(2)$
$\alpha_{3000,1}$, $cm^{-2}\cdot bar^{-1}$	22,72	18,59	2,048	1,583	0,036	8,598	0,513
ω_0, cm^{-1}	1594	3700	5340	7240	9100	3569	6953
λ_0, μ	6,3	2,7	1,87	1,38	1,1	2,8	1,44
$\Delta\omega_s$, cm^{-1}	0	0	0	0	0	461	230
a, cm^{-1}	502	502	504	502	502	673	570
δ	1	1	1	1	1	0	0

Parameter	$CO_2(1)$	$CO_2(2)$	$CO_2(3)$	$CO(1)$	$CO(2)$	H_2	$NO(1)$	$NO(2)$
$\alpha_{3000,1}$, $cm^{-2}\cdot bar^{-1}$	269,2	14,96	1,092	21,3	0,282	0,207	9,759	0,421
ω_0, cm^{-1}	2349	3716	5109	2143	4258	4500	1876	3700
λ_0, μ	4,3	2,7	1,96	4,7	2,35	2,22	5,33	2,7
$\Delta\omega_s$, cm^{-1}	49	41	36	208	105	0	160	80
a, cm^{-1}	396	407	472	219	218	466	204	200
δ	0	0	0	0	0	1	0	0

Thrust Chamber Outer Cooling

Radiation Cooling

The general steady-state heat transfer equation for the cooled thrust chamber can be expressed as follows:

$$q_w^{T_{wg}} + q_r^{T_{wg}} = \frac{\lambda_w}{t_w}(T_{wg} - T_{wc}) = \varepsilon_{wc}\sigma T_{wc}^4 = q_{rc}^{T_{wc}}$$

where

$q_w^{T_{wg}}$ and $q_r^{T_{wg}}$ – convective and radiation heat flux to the inner surface of the wall at the temperature T_{wg} ;

$q_{rc}^{T_{wc}}$ – radiation heat flux from the outer surface of the wall at the temperature T_{wc} ;

T_{wg} – temperature on the inner surface of the wall;

T_{wc} – temperature on the outer surface of the wall;

$\sigma = 5.670373 \times 10^{-8} \quad W/(m^2 K^4)$ – Stefan–Boltzmann constant;

ε_{wc} – emissivity coefficient of the wall material (see Table 1 for typical values of some materials);

λ_w – thermal conductivity of the wall at the temperature $T = 0.5(T_{wg} + T_{wc})$;

t_w – thickness of the wall.

The steady-state heat transfer at each chamber/nozzle station is solved iteratively and finishes when both T_{wg} and T_{wc} are found such that the heat flux to the inner surface of the wall $(q_w^{T_{wg}} + q_r^{T_{wg}})$ is equal to the heat flux from the outer surface $q_{rc}^{T_{wc}}$.

Regenerative Cooling

For the numerical procedure, the thrust chamber is subdivided into a number of stations along the longitudinal direction *L*, as shown in figure 3.

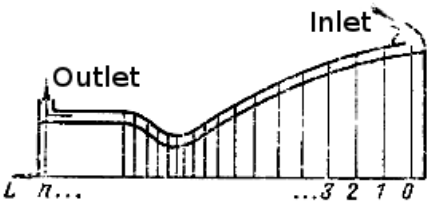

Figure 3: A thrust chamber subdivided into a number of stations

The temperature distribution within the wall is determined via an space-marching technique starting from station 0 to the last station *n*. The program marches axially from one station to another. At each station, the following set of equations is used to determine the temperature of the thrust chamber wall:

$$(q_w^{T_{wg}} + q_r^{T_{wg}}) A_w = \dot{m}_c \bar{c}_c (T_c^{\text{out}} - T_c^{\text{in}})$$

$$d T_c = \frac{2\pi R (q_w^{T_{wg}} + q_r^{T_{wg}})}{\dot{m}_c \bar{c}_c} dx$$

$$q_w^{T_{wg}} + q_r^{T_{wg}} = \frac{\lambda_w}{t_w} (T_{wg} - T_{wc})$$

$$q_w^{T_{wg}} + q_r^{T_{wg}} = \alpha_c (T_{wc} - T_c) = q_{wc}^{T_{wc}}$$

$$\alpha_c = Nu \frac{\lambda_c}{d_e}$$

$$Nu = 0.021 \,\mathrm{Re}_c^{0.8} Pr_c^{0.4} \left(0.64 + 0.36 \frac{T_c}{T_{wc}}\right)$$ (for kerosene) [2]

$$Nu = 0.033 \,\mathrm{Re}_c^{0.8} Pr_c^{0.4} \left(\frac{T_c}{T_{wc}}\right)^{0.57}$$ (for liquid hydrogen) [2]

$$Nu = 0.0185 \,\mathrm{Re}_c^{0.8} Pr_c^{0.4} \left(\frac{T_c}{T_{wc}}\right)^{0.1}$$ (for methane) [2]

$$Nu = 0.023 \,\mathrm{Re}_c^{0.8} Pr_c^{0.4}$$ (for other coolants) [1]

where

$q_w^{T_{wg}}$ and $q_r^{T_{wg}}$ – convective and radiation heat flux to the inner surface of the wall at the temperature T_{wg}

T_{wg} – gas-side wall temperature

T_{wc} – coolant-side wall temperature

λ_w – thermal conductivity of the chamber wall at the temperature $T = 0.5(T_{wg} + T_{wc})$

t_w – thickness of the chamber wall

T_c – coolant temperature

T_c^{in} – initial temperature of the coolant as it enters the station

T_c^{out} – final temperature of the coolant as it leaves the station

$\bar{c}_c$ – average coolant specific heat

$\dot{m}$ – coolant mass flow rate

A_w – wall surface area

d_e – equivalent diameter of the cooling passage

The calculation of the temperature distribution is performed iteratively as follows:

1. Subdivide the thrust chamber into several stations (see figure 3).
2. On the first iteration step $(i = 0)$, assign the initial gas-side temperatures $T_{wg}^{(i=0)}$ at

each station.

3. At each station, calculate the gas-side heat flux (convective and radiation) for given $T_{wg}^{(i)}$; in order to improve the execution speed of the program, the Ievlev's correlation for similar conditions can be used on the follow-up iteration steps $(i>0)$ (see section Boundary Layer Cooling).

4. At each station, calculate the coolant heating and coolant exit temperature for known input temperature (the direction of space-marching depends on the coolant flow direction).

5. Calculate the coolant-side heat transfer coefficient α_c .

6. From known heat flux and coolant-side heat transfer coefficient, calculate new values of the coolant-side temperature $T_{wc}^{(i+1)}$ and the gas-side temperature $T_{wg}^{(i+1)}$.

7. Calculate the convergence criteria as $\delta=\frac{|T_{wg}^{(i)}-T_{wg}^{(i+1)}|}{T_{wg}^{(i)}} < 0.05\,T_{wg}^{(i)}$.

When the present iteration step is completed, comparison is made between the results of the present step and that of the previous one to see if the convergence criteria has been met. If it is not met at least at one station, the calculation starts again. The process continues until the convergence is achieved at all stations.

Pressure Drop in Cooling Passages

The cooling passage can be treated as a hydraulic conduit and the pressure drop calculated accordingly, as follows [7]:

$$\Delta p=\lambda\frac{l}{d_e}\rho\frac{w^2}{2}$$

where

λ – friction loss coefficient, a function of the Reynolds number and of cooling passage conditions such as geometric shape, surface smoothness etc.

l – length of the cooling passage

$d_e=4A/\Pi$ – equivalent average diameter of the cooling passage

ρ – average density of the coolant

$w=\dot{m}/\rho A$ – coolant flow velocity

$\dot{m}$ – coolant total mass flow rate

A – average total cross-section area of the cooling passages (that is the sum of the cross-sections of all passages at specific station)

Π – average total perimeter of the cooling passages (that is the sum of the perimeters of all passages at specific station)

Friction loss coefficient is estimated as follows [4], [7]:

– for laminar flows (Re ≤ 2320): $\lambda = \frac{64}{\mathrm{Re}} \varepsilon_f$

– for turbulent flows (2320 < Re < 10^5): $\lambda = \frac{0.3164}{\sqrt[4]{\mathrm{Re}}} \varepsilon_f$

– for turbulent flows (Re > 10^5): $\lambda = \left(0.0032 + \frac{0.221}{\mathrm{Re}^{0.237}} \right) \varepsilon_f$

Coefficient ε_f depends on geometric shape of the coolant passages and is given in the sections below.

Coaxial-Shell Thrust Chamber Design

Regenerative cooling in coaxial-shell thrust chambers can be performed directly as described in the previous sections.

Coefficient for calculation of the pressure drop is given as: $\varepsilon_f = 1.5$ [4]

Channel-Wall Thrust Chamber Design

Regenerative cooling in channel-wall thrust chambers can be performed as described in previous sections with following deviations [4]:

$$\alpha_c = \eta_r Nu \frac{\lambda_c}{d_e}$$

$$\eta_f = \frac{a}{a+\delta} + \frac{2b}{a+\delta} \frac{th\xi}{\xi}$$

$$\xi = \sqrt{\frac{2\alpha_c \delta}{\lambda_w}} \frac{b}{\delta}$$

where

η_f – coefficient, introduced to reflect the increase in surface area of the cooling passages (fin effect)

a , b , δ – width and height of the channel and thickness of the fin correspondingly

α_c – coolant-side heat transfer coefficient

λ_w – thermal conductivity of the wall and fins

Coefficient ε_f depends on the shape of the single channel and can be estimated from the figure 5.

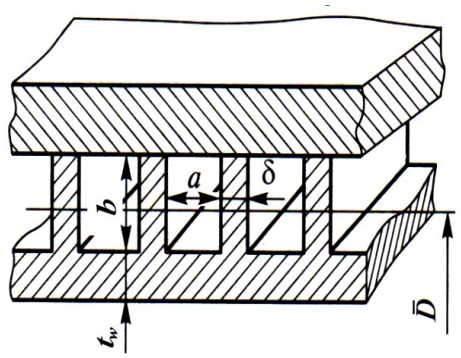

Figure 4: Channel-wall thrust chamber schematic

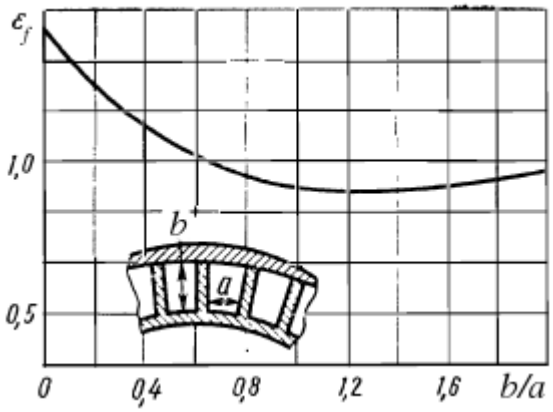

Figure 5: Form factor for channel-wall design [6]

Tubular-Wall Thrust Chamber Design

Regenerative cooling in tubular-wall thrust chambers can be performed as described in section Channel-Wall Thrust Chamber Design with following deviations [4]:

- coefficient for calculation of the pressure drop is given as:
  - for cooling passages with circular cross section $\varepsilon_f \approx 1$
  - for cooling passages with non-circular cross section the coefficient ε_f can be estimated from figure 5.
- coefficient η_f is calculated in the same way as described before, obtaining parameters a , b and δ as shown in figure 6.

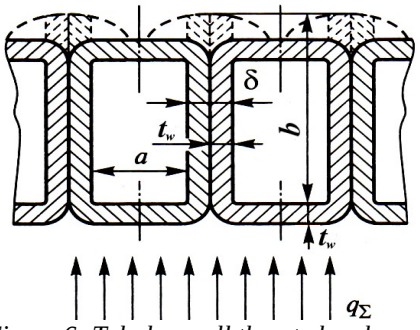

Figure 6: Tubular-wall thrust chamber schematic

Thermal Barrier Coating Layer

The thermal barrier coating (TBC) is used to reduce the temperature gradient across the chamber wall.

The functional principle of a TBC, illustrated in figure below, is to increase the hot gas side wall temperature T_{wg}. This is achieved by applying a ceramic top layer (e.g. Y2O3-stabilized ZrO2, PYSZ) onto the wall base material. The PYSZ ceramic offers a thermal conductivity λ of about 1.5 W/(m K). In order to prevent a coating overheat (>1500 K) coating thicknesses of less than 0.1 mm are required. These high hot gas side wall temperatures compared to the maximum temperatures of the wall without coating lead to the significant reduction in heat flux.

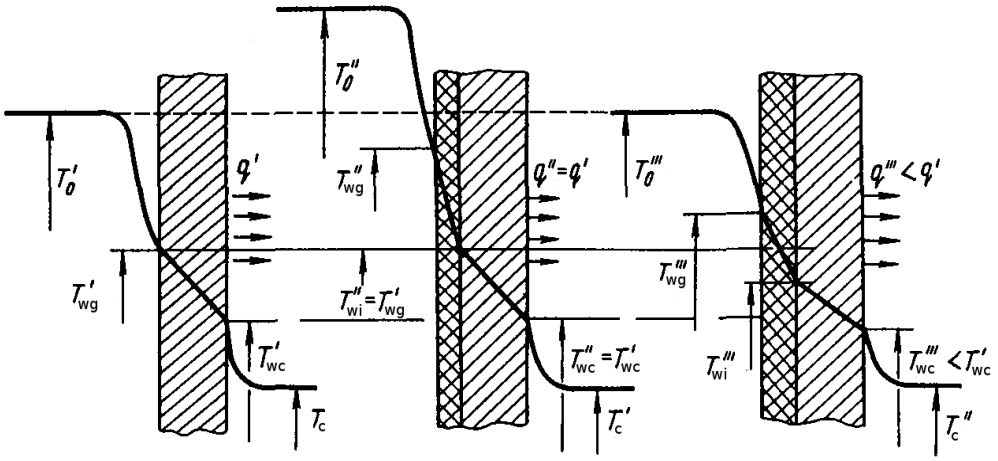

Figure 7: Functional principle of a TBC

With such a protective layer, the application range of existing regenerative or radiation cooling thrust chambers can be enlarged towards higher combustion chamber pressures or an increased thrust chamber life.

In general a TBC acts as an insulator to the inner liner, reducing the wall heat flux into the wall base material.

For the analysis of thrust chambers with TBC the following equation is used:

$$q_w^{T_{wg}} + q_r^{T_{wg}} = \frac{1}{\frac{t_1}{\lambda_1} + \frac{t_2}{\lambda_2} + \ldots + \frac{t_N}{\lambda_N}} (T_{wg} - T_{wc})$$

where

$t_1, t_2, \ldots, t_N$ – thicknesses of TBC layers and the base wall

$\lambda_1, \lambda_2, \ldots, \lambda_N$ – thermal conductivities of TBC layers and the base wall

Loss in Specific Impulse

Loss in specific impulse due to friction in boundary layer is calculated using following relations [8]:

$$\xi_f = \frac{2\pi \int_0^{x_e} \tau R \cos\theta \, dx}{C_f^i A_t p_c^0}$$

$$\varphi_f = 1 - \xi_f$$

where

ξ_f – friction loss coefficient

φ_f – performance correction factor for the friction loss

τ – viscosity stress (see section “Gas-Side Heat Transfer”)

C_f^i – ideal thrust coefficient

A_t – nozzle throat area

p_c^0 – stagnation pressure at nozzle inlet

x , R , θ – size and shape parameters of the thrust chamber as defined in figure 1

Computer Program RPA

The described numerical model has been implemented in the computer program RPA.

Graphical User Interface

Input Data

The screen Thermal Analysis consists of 3 tabs *Heat Transfer Parameters*, *Thrust Chamber Cooling* and *Thermal Analysis*.

On the tab *Heat Transfer Parameters* the user can define heat transfer parameters used to calculate the heat transfer rate distribution in the thrust chamber (figure 8).

On the tab *Thrust Chamber Cooling* the user can define design parameters of thrust chamber cooling (figure 9). On this screen the user can add new cooling sections and define their parameters.

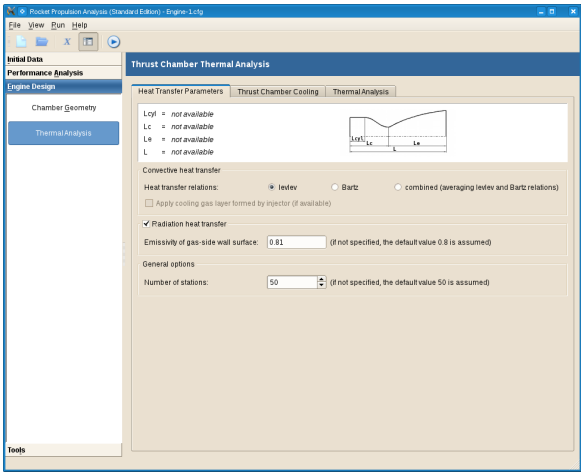

Figure 8: Heat Transfer Parameters

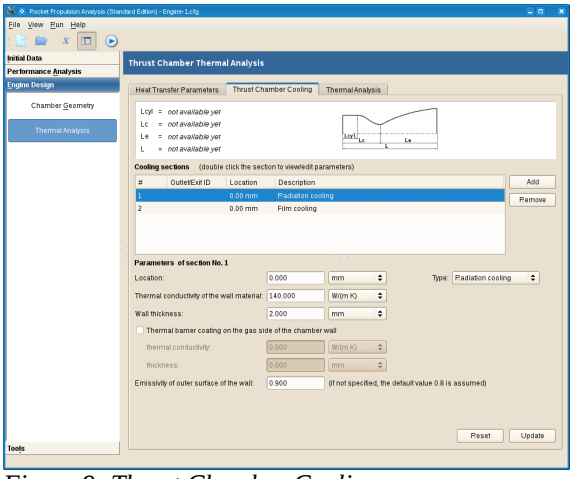

Figure 9: Thrust Chamber Cooling

Output Data

After specifying all required parameters and starting the analysis, the user can see the results on the tab *Thermal Analysis* (figure 10).

The thrust chamber geometry is printed out in columns "Location" and "Radius".

The column "Heat flux" displays the calculated heat flux (depending on heat transfer parameters, either the sum of convection heat flux and radiation heat flux or convection heat flux only) at the corresponding location.

The column "T_{wg}" displays the temperature of

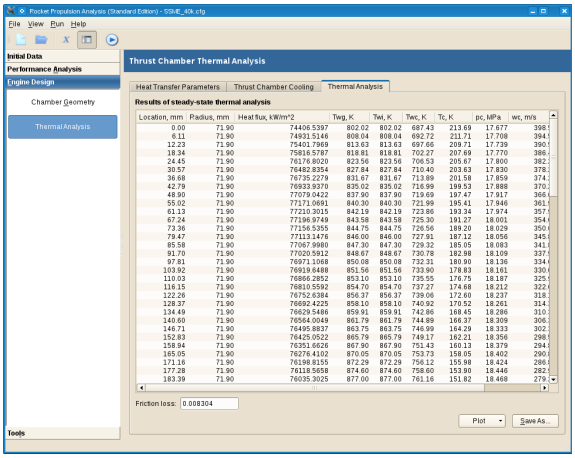

Figure 10: Thermal analysis results

chamber wall on its hot gas side.

The column "T_{wi}" displays the temperature between the thermal barrier coating layer and chamber wall (if coating is available) or the temperature of chamber wall on its hot gas side (the same as T_{wg}).

The column "T_{wc}" displays the temperature of chamber wall on its cold side.

The columns "T_c" and "wc" display the temperature and the velocity of the coolant (if applicable).

Using context menu, the user can copy the content of the complete table or single selected row into the clipboard.

The user can plot the the diagrams "Heat Flux vs. Location" or "Temperatures vs. Location", clicking the button Plot at the bottom-right corner of the tab. The location of nozzle throat is shown on the diagram by corresponded vertical marker line (figures 11,12).

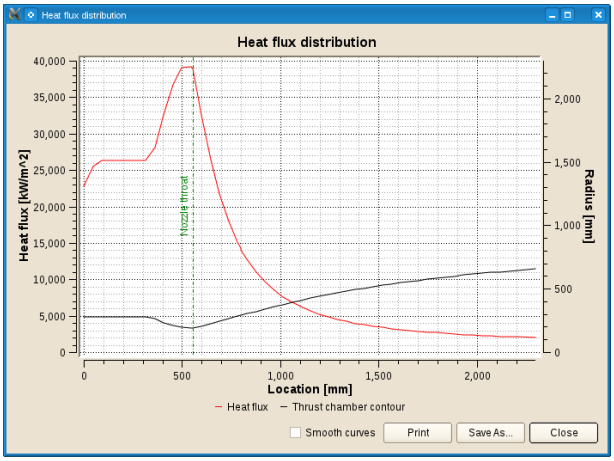

Figure 11: Diagram „Heat flux vs. Location“

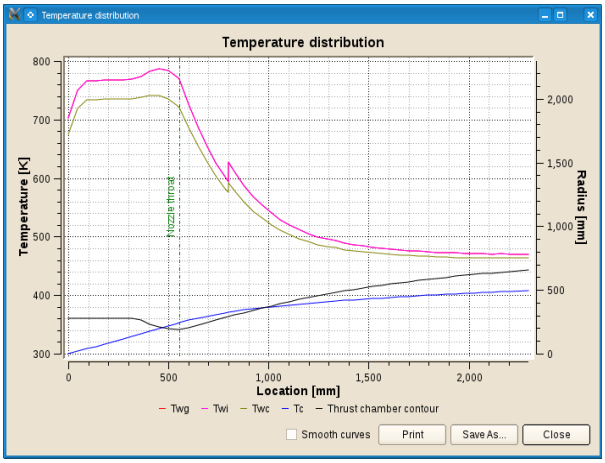

Figure 12: Diagram „Temperatures vs. Location“

Verification

To verify the accuracy of the thermal analysis module of RPA, the comparison between available reference data and RPA prediction has been performed.

The obtained agreement between the RPA prediction and referenced data is sufficient for the tool used in conceptual and preliminary design studies (phase 0/A/B1).

Quantitative and qualitative differences in results can be explained by the following:

- RPA does not simulate fuel atomization and dispersion, as well as droplets burning.
- The hot gas properties for thermal analysis are retrieved from the quasi one-dimensional flow model.
- The heat transfer is simulated using semi-empirical relations.

SSME 40k

Design parameters [10]

	40 K water cooled	40 K regeneratively cooled	
Parameter	**Value**	**Value**	**Unit**
Components mass ratio	6.0	6.0	O/F
Combustion chamber pressure	10.87	20.47	MPa
Combustion chamber diameter	43.8	43.8	mm
Contraction ratio	2.92	2.92	-
Chamber length (L')	355.6	355.6	mm
Nozzle exit area ratio	7	5	A_e/A_t

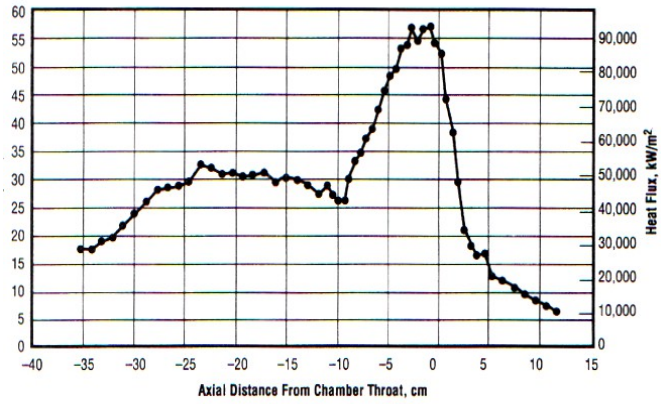

Figure 13: SSME 40 K calorimeter chamber heat flux profile [10]

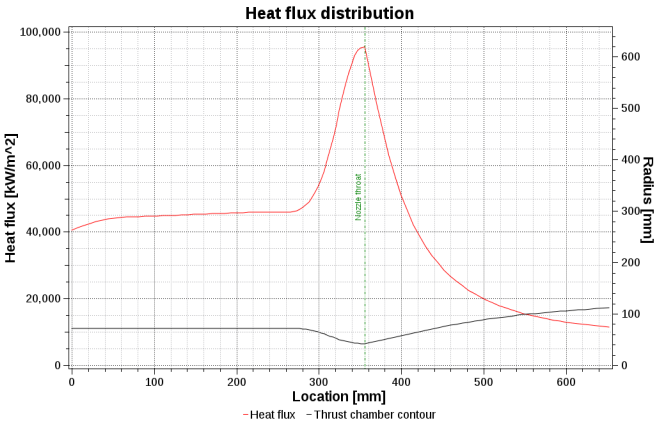

Figure 14: SSME 40 K calorimeter chamber heat flux profile, predicted by RPA

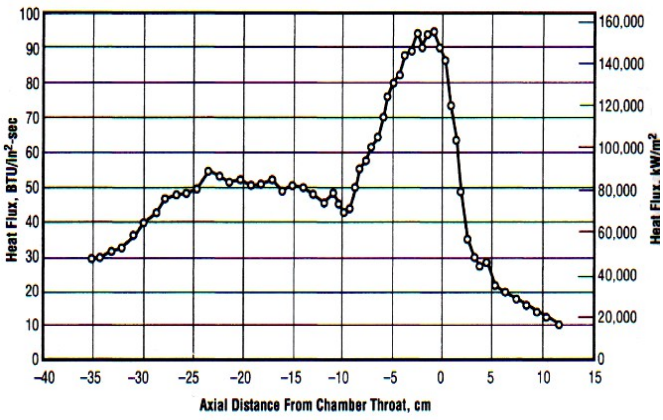

Figure 15: SSME 40 K regenerative chamber predicted heat flux profile [10]

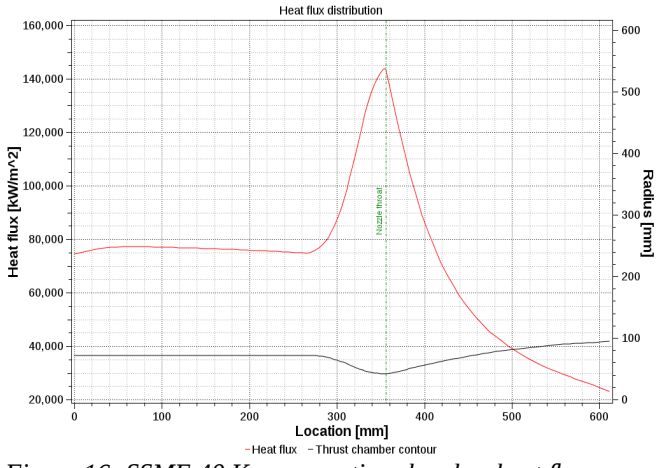

Figure 16: SSME 40 K regenerative chamber heat flux profile, predicted by RPA

Aestus

Design parameters (reference load point R) [11]

Parameter	*Value*	*Unit*
Oxidizer	NTO (N_2O_4)	-
Fuel	MMH	-
Components mass ratio	2.05	O/F
Combustion chamber pressure	10.3	bar
Combustion chamber diameter	210	mm
Nozzle throat diameter	136	mm
Chamber length (L')	310	mm
Length of regeneratively cooled chamber	591	mm
Nozzle exit area ratio	84	A_e/A_t

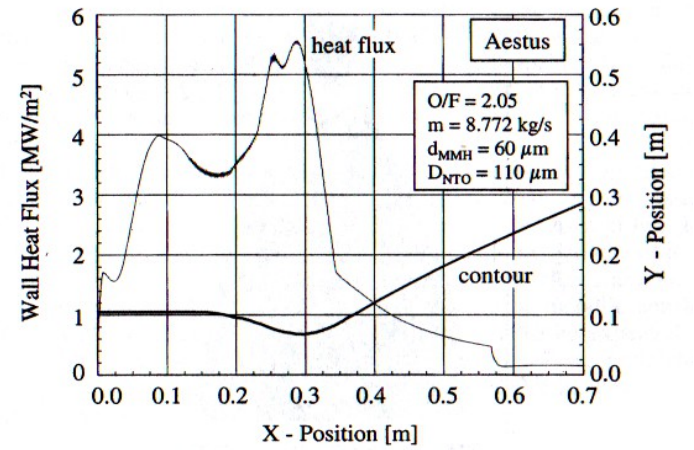

Figure 17: Calculated heat flux distribution [11]

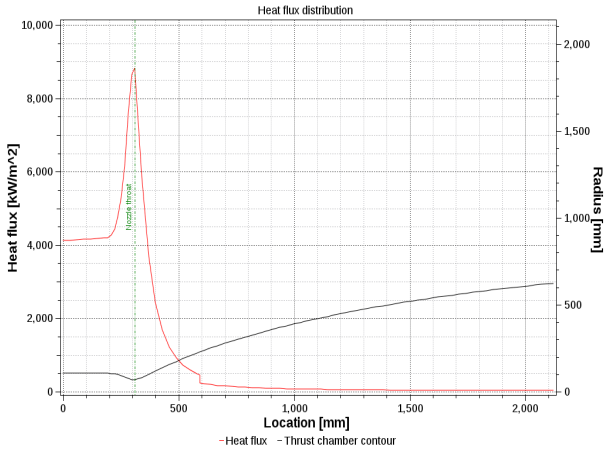

Figure 18: Calculated heat flux distribution, predicted by RPA

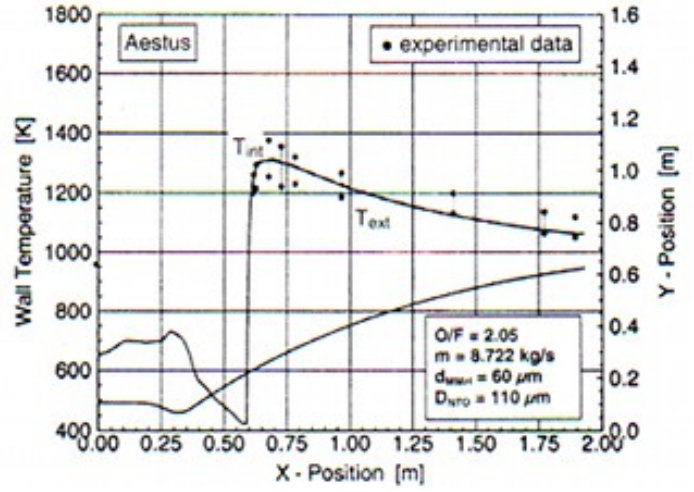

Figure 19: Temperature distribution [11]

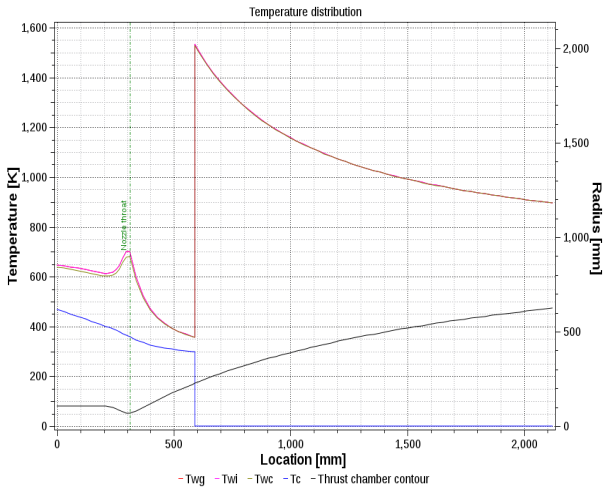

Figure 20: Temperature distribution, predicted by RPA

Future Work

The capabilities of Thermal Analysis Module for RPA will continue to be expanded upon. Enhancements currently being developed include:

- Implementing the calculation of hot gas properties for the thermal analysis using axisymmetric method of characteristics, replacing the present quasi one-dimensional flow model.
- Refinement of the model for the film cooling analysis.
- Refinement of the models for the regenerative cooling analysis.
- Improved user interface to allow more flexible.
- Improved execution speed.

Conclusion

Thermal Analysis Module for RPA, a commercially available product, has been introduced to the space propulsion community to assist in the design of liquid-propellant rocket engines. This modern tool is suitable for use in conceptual and preliminary studies. Its friendly graphical user interface and its ergonomics respond to the needs of flexibility and easy of use in the daily activity. The tool has been executed and shown to be in good agreement with published data.

References

1. Vasiliev A.P., Kudryavtsev V.M. et al. Basics of theory and analysis of liquid-propellant rocket engines, vol.2. 4th Edition. Moscow, Vyschaja Schkola, 1993. (in Russian)

2. Lebedinsky E.V., Kalmykov G.P., et al. Working processes in liquid-propellant rocket engine and their simulation. Moscow, Mashinostroenie, 2008. (in Russian)

3. Huzel, D.K., Hwang, D.H., Modern Engineering for Design of Liquid Rocket Engines, ISBN 1-56347-013-6, American Institute of Aeronautics and Astronautics, 1992.

4. Dobrovolsky M.B. Liquid-propellant rocket engines. 2nd Edition. Moscow, Bauman MSTU, 2005. (in Russian)

5. Sutton, G.P. and Biblarz, O. Rocket Propulsion Elements, 7th Edition. John Wiley & Sons, 2001.

6. Babkin A.I., Belov S.I., et al. Basics of theory of automatic control of rocket engines. Moscow, Mashinostroenie, 1986. (in Russian)

7. Katorgin B.I., Kiselev A.S., Sternin L.E., Chvanov V.K. Applied gas dynamics. Moscow, Vusovskaja kniga, 2009. (in Russian)

8. Kurpatenkov V.D., Kesaev Kh.V. Analysis of thrust chamber of liquid-propellant rocket engine. Moscow, MAI, 1993. (in Russian)

9. Ponomarenko A. RPA: Tool for Liquid Propellant Rocket Engine Analysis. 2010.

10. Carol E. Dexter, Mark F. Fisher, James R. Hulka, Konstantin P. Denisov, Alexander A. Shibanov, and Anatoliy F. Agarkov. Scaling Techniques for Design, Development, and Test. Liquid Rocket Thrust Chambers - Aspects of Modeling, Analysis, and Design - Progress in Astronautics and Aeronautics, Volume 200.

11. Dieter Preclik, Oliver Knab, Denis Estublier, and Dag Wennerberg. Simulation and Analysis of Thrust Chamber Flowfields: Storable Propellant Rockets. Liquid Rocket Thrust Chambers - Aspects of Modeling, Analysis, and Design - Progress in Astronautics and Aeronautics, Volume 200.